Astron. Astrophys. 323, 177–182 (1997)

ASTRONOMY
AND
ASTROPHYSICS

# A spectral analysis of the hydrogen-deficient star HD144941

**P.M. Harrison and C.S. Jeffery**

School of Physics and Astronomy, University of St Andrews, North Haugh, St. Andrews, Fife, KY16 9SS, Scotland

Received 2 April 1996 / Accepted 2 July 1996

**Abstract.** HD144941 is a B type hydrogen-deficient star. Previous analysis has suggested that its effective temperature and surface gravity are similar to the nitrogen rich H-deficient star V652 Her. However, its H/He ratio puts it between the classifications of an extreme and an intermediate helium star, and its low C and N abundances make it unique amongst known H-deficient stars.

High-resolution, high-S/N, optical spectra have been obtained using the AAT. A grid of model atmospheres has been constructed for varying $T_{\rm eff}$, $\log g$ and H/He abundance. Ionisation equilibria for available metal ions, fitted He I line profiles, and UV/visual flux distributions have been used to determine $T_{\rm eff}$, $\log g$ and H/He.

With optimal values of $T_{\rm eff}$ = 23 200 K and $\log g$ = 3.9 the abundances by number of the principal species are: $n_{\rm H}$ = 5.21 %, $n_{\rm He}$ = 94.79 %, $n_{\rm C}$ = 0.0017 %, $n_{\rm N}$ = 0.00079 %, $n_{\rm O}$ = 0.0024 %, $n_{\rm Mg}$ = 0.00031 %, $n_{\rm Al}$ = 0.000019 %, $n_{\rm Si}$ = 0.00027 %, $n_{\rm Fe}$ = 0.00066 %.

HD144941 lies at the high $\log g$, high $T_{\rm eff}$ end of the group of EHe stars, but its $n_{\rm H}/\,n_{\rm He}$ ratio of 0.055 is above average for the group. The surface composition is also remarkable in having a considerable metal deficiency (Z=0.0003), probably of primordial origin.

The low metallicity explains why substantial radial pulsations are not observed for a star with these surface properties and is a vindication of modern helium star pulsation models and opacities.

**Key words:** stars: helium stars – individual stars (HD144941) – atmospheres – abundances – oscillations – evolution

## 1. Introduction

HD144941 is a 10th magnitude star of spectral type B8. It was found to be hydrogen-deficient in a spectral survey of the southern sky by MacConnell et al. in 1970. The star was also found to have a large radial velocity and high galactic latitude characteristic of an old population.

*Send offprint requests to*: P.M. Harrison

In an analysis of low resolution spectra, Hunger and Kaufmann (1973) found the $n_{\rm H}/\,n_{\rm He}$ ratio to be 0.1. They noticed that this ratio placed HD144941 between the classifications of extreme ($n_{\rm H}/\,n_{\rm He}$ = $10^{-3}$) and intermediate ($n_{\rm H}/\,n_{\rm He}$ = 1) hydrogen deficient (H-def) stars. They found the effective temperature $T_{\rm eff}$ = 21.5 kK and the surface gravity $\log g$ = 3.5. The analysis also showed an under-abundance of C and N with respect to typical B-stars. Other metal lines were so weak as to be undetectable on the spectrum available to them. To measure the metallicity accurately, high-resolution, high-S/N spectra would be required. In a study of He-rich B-stars Osmer and Peterson (1974) found similar values for the photospheric parameters. In both analyses LTE models with no line blanketing were used. A recent study of low-S/N spectra using line blanketed models (Dundas & Jeffery, unpublished) found $T_{\rm eff}$ and $\log g$ to be higher than previous values, prompting a further study using higher S/N data.

The question arises as to whether HD144941 is an intermediate helium star, related to chemically peculiar main sequence B stars (Hunger & Kaufmann 1973), an extreme helium star (EHe), representing a high-H, high-g extension to the group which includes HD124448 (Drilling 1986), or the unrecognised prototype of a recently defined group of helium-rich subdwarf B-stars (HesdB, Moehler et al. 1990). Note that both EHes and HesdBs are characterised by strong lines of He I and weak or absent H Balmer lines and He II 4686 Å.

It is clear that HD144941 exhibits unusual surface abundances. It is important to determine whether they are primarily the result of evolutionary processes or whether other atmospheric processes have played a significant rôle. Data on additional species (e.g. Si, Fe) is required to discriminate between possible scenarios.

Finally, HD144941 has surface properties ($T_{\rm eff}$, $\log g$) similar to two EHes, V652 Her (Lynas-Gray et al. 1984) and LSS3184 (Drilling et al. 1996). These stars are observed to be variable with periods of 0.1 day caused by radial pulsations. Jeffery & Hill (1996) recently reported no significant variability for HD144941 on the timescales that would be expected due to radial pulsations. The following analysis provides an explanation of why HD144941 is not a radial pulsator.

## 2. Observations

### *2.1. Optical spectroscopy*

The observations used for the analysis consisted of optical échelle spectra obtained in the blue spectral region using a TEK1024 CCD with the University College London échelle spectrograph (UCLES) on the Anglo-Australian Telescope (AAT) on 15/16 April 1995.

The raw échelle spectra were reduced (ie bias subtracted, flat-fielded, extracted and wavelength calibrated) using the Starlink software packages Figaro and Echomop to produce calibrated échellograms. The rectification of the blaze and detector response functions, the normalisation of the stellar continuum, the merging of the échelle orders and the co-adding of resultant spectra were carried out using the authors' purpose-designed software.

Additionally, a low resolution spectrum in the range 3880 Å to 4550 Å obtained on the 1.9m RPCS at the South African Astronomical Observatory (SAAO) in May 1988 was used. This spectrum has a dispersion of 0.4 Å $\mathrm{px}^{-1}$ and a mean S/N of approximately 60 and has been normalised as a single spectrum across its whole range. The difficulties involved in determining continuum and normalising the AAT échelle orders were minimized by normalising them to the SAAO spectrum.

The result of the reduction is a single spectrum of HD144941 in the range 3840 Å to 4960 Å with a dispersion of 0.1 Å $\mathrm{px}^{-1}$ and S/N $\approx$ 120.

The final spectrum is shown in Fig. 1, where it is compared with V652 Her (Jeffery & Hill, in preparation), LSS3184 (Drilling et al. 1996) and PG1544+488 (Heber et al. 1988). Three features are immediately apparent in the spectrum of HD144941. The comparative strength of the Balmer lines, the weakness of the metal lines, and the richness of the He I spectrum. The latter is remarkable since, in addition to the familiar forbidden component [He I]$\lambda$4469.9 Å frequently seen in EHes, we have identified all forbidden He I lines in the observed wavelength region. The significance of the [He I] lines is that their sensitivity to density means they can provide a vital $\log g$ diagnostic. The resolution and S/N of the final spectrum allowed lines to be detected with $W_\lambda = 8 \pm 1m$ Å with errors (1 $\sigma$) in $W_\lambda$ typically $\pm 10\%$. All identified lines for which atomic data was available had their equivalent widths determined (Table 1).

### *2.2. Ultraviolet and optical spectrophotometry*

Flux calibrated ultraviolet spectra of HD144941 were obtained with the International Ultraviolet Explorer (IUE) in the wavelength range 1200 Å to 3200 Å. The spectrum used was obtained from the IUE archive and is summarised by Jeffery et al. (1986).

These were supplemented by optical uvby photometry obtained at the SAAO (Jeffery & Hill 1996).

## 3. Analysis

### *3.1. The model atmospheres and theoretical line profiles*

A grid of photospheric models was computed using the stellar atmosphere code most recently described by Jeffery and Heber (1992). This LTE code includes continuous opacity sources due to Thompson and Rayleigh scattering as well as bound free transitions of principal species as described by Kurucz (1970) and Peach (1970). Also the effects of line-blanketing could be included using opacity distribution functions for a hydrogen-deficient mixture calculated by Möller (1990). The grid was calculated for varying $T_{\rm eff}$ and $\log g$ with $n_{\rm H}$ = 0.05 (similar to that found in previous analyses). The microturbulent velocity was set to 10 km $\mathrm{s}^{-1}$ after the C II$\lambda$1324 Å line analysis of Jeffery et al. (1986).

Line formation calculations were carried out using the spectrum-synthesis code developed at Belfast by Dufton, Lennon and Conlon. This LTE code initially designed for B-star atmospheres was extended to treat H-deficient atmospheres by Jeffery and Heber (1992).

### *3.2. The method of fine analysis*

The method of fine analysis has been applied to the spectrum of HD144941 in order to determine values for the surface parameters. The analysis was first conducted using line blanketed models with solar abundances. The results of this initial analysis (Harrison and Jeffery 1996) revealed a very low metallicity.

A defect of the initial analysis was an inconsistency of 800K between the ionisation equilibrium temperature and that given by the observed flux distribution. Since the available opacity distribution function was calculated for a solar metallicity, the analysis was repeated using models calculated with continuum opacities only. In this case the two temperature diagnostics were found to coincide.

*He I line profile fitting.* Line profiles were calculated for a number of diffuse He I lines for each of the models. For several values of $T_{\rm eff}$ a $\log g$ was determined for which the synthetic line matched the observed data (e.g. see Fig. 2). This was used to determine $\log g$ as a function of $T_{\rm eff}$. The fit could not be made exactly due to incorrect modelling of the core of the line probably caused by non-LTE effects in the outer layers of the photosphere (see Jeffery & Heber 1992). The wings of the diffuse lines were hence used as indicators of the correct gravity. The low H and metal abundances for this star mean that He I lines are relatively free of blends with other species. However, as described earlier, all forbidden lines of He I are present in the spectrum. Since they frequently disturb the profile of the diffuse He I lines used to measure $\log g$, it is only possible to use those lines for which the theoretical profiles include the forbidden components. In practice the adopted profiles due to Barnard et al. (1969, 1974, 1975) include the forbidden components He I$\lambda$ 4469.9, 4517.4, 4920.4 and 4910.7 Å. Whilst these have provided useful $\log g$ constraints, modern data for

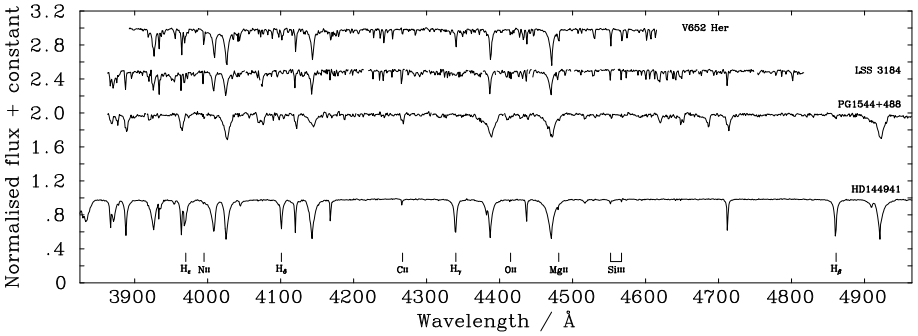


**Fig. 1.** The final spectrum of HD144941, binned to 1 Å px$^{-1}$ to compare with V652 Her (Jeffery et al. 1986), LSS3184 (Drilling et al. 1996) and PG1544+487 (WHT UES, 1995). Major non-He I absorption lines are indicated

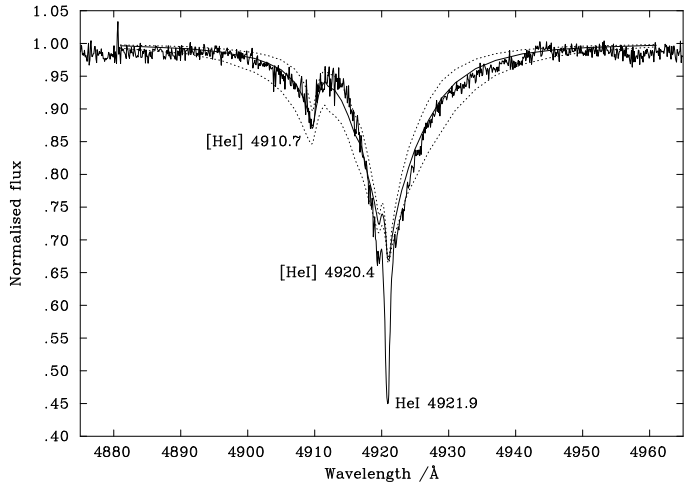


**Fig. 2.** He I$\lambda$4921 Å line profiles: AAT data (jagged solid line), final model ($T_{\rm eff}$ = 23.2kK, $\log g$ = 3.9, smooth solid line), model ($T_{\rm eff}$ = 23.2kK, $\log g$ = 4.5, lower dotted line), model($T_{\rm eff}$ = 23.2kK, $\log g$ = 3.5, upper dotted line)

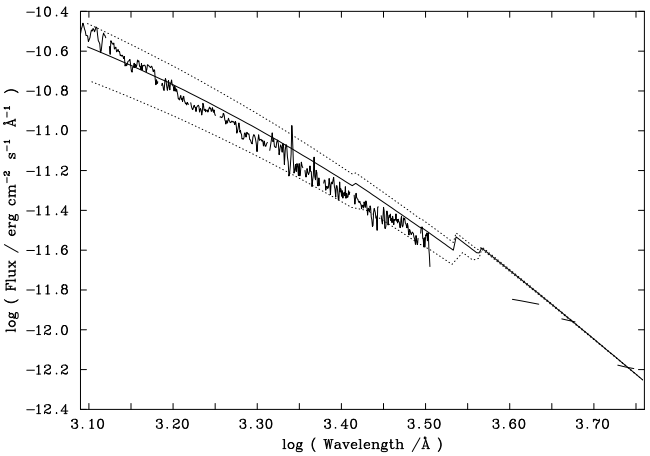


**Fig. 3.** The dereddened ($E_{\rm B-V}$ = 0.25) UV flux distribution for HD144941 (jagged solid line) compared with the final model ($T_{\rm eff}$ = 23.2kK, $\log g$ = 3.9, smooth solid line) and the models ($T_{\rm eff}$ = 26kK, $\log g$ = 4.0, upper dotted line) and ($T_{\rm eff}$ = 20kK, $\log g$ = 4.0, lower dotted line)

additional lines (cf. Beauchamp et al. 1996) should be used in future.

*Ionisation equilibria.* Equivalent widths of the absorption lines of prominent ions were used in the line formation code to find the respective abundances for each of the models. For each $\log g$ the $T_{\rm eff}$ was found for which the abundances given by two ions of the same element agreed. This method of finding ionisation equilibria was used to determine $T_{\rm eff}$ as a function of $\log g$.

*Flux distribution* A grid of model flux distributions was calculated for varying $T_{\rm eff}$ and interstellar extinction. The UV/optical data was dereddened using Seaton's (1979) galactic reddening law.

The value $E_{\rm B-V}$ = 0.25 was found by fitting the dereddened data at the $\lambda$2200 Å interstellar absorption feature to the unreddened model. The adopted temperature was found using a method following that described by Underhill (1982). In this method the observed integrated flux and model integrated flux are compared between two wavelength limits (in this case 1210 and 5560 Å). The ratio of the unnormalised observed flux to the model flux gives the angular diameter. The ratio of the model flux over all wavelengths to that inside the wavelength range being considered gives a corrective factor to the observed flux which allows an estimate of the total flux. The angular diameter and total flux can then be used to calculate $T_{\rm eff}$.

### *3.3. Final model*

Loci for the He I line profile fits, ionisation equilibria and flux distribution fit were plotted in $T_{\rm eff}$–$\log g$ space (Fig. 4). The intersect of the loci was used to determine optimum values of $T_{\rm eff}$ and $\log g$. Finally the H abundance was calculated from Balmer line equivalent widths (H $\beta$, H $\gamma$, H $\delta$) and C, N and O abundances were calculated from available equivalent widths. The entire procedure was then iterated, using derived abundances as input to the model atmosphere calculations, until a final model atmosphere was obtained.

The final model obtained is described by $T_{\rm eff}$ = 23200 $\pm$ 500 K, $\log g = 3.9 \pm 0.2$, $v_{\rm t}$ = 10 km s$^{-1}$ and $n_H$ = 5 % (relative abundance by number), where errors in $T_{\rm eff}$ and $\log g$ are 3$\sigma$ values (all observed diagnostics). The abundances of all identifiable species (Table 2) were derived from their equivalent widths. Errors are obtained as standard deviations from all lines in Table 1, or estimated from the error range in the equivalent widths.

**Table 1.** Equivalent widths and relative abundances for significant absorption lines. Species and multiplets considered were selected for $W_\lambda \geq 8$ mÅ. They are shown here if they are free of blending with other species and atomic data was available. References for gf values are given with the ion designation

| Ion Mult. | $\lambda$/ Å | $W_\lambda$ / mÅ | Reference $\log gf$ | $-\log n$ |
|---|---|---|---|---|
| $H_\delta$ | 4101.74 | 1690 | | 1.33 |
| $H_\gamma$ | 4340.47 | 1830 | | 1.26 |
| $H_\beta$ | 4861.3 | 1835 | | 1.19 |
| He I | | | | |
| 60 | 3871.82 | 1830 | | |
| 58 | 3926.50 | 2920 | | |
| 5 | 3964.73 | 660 | | |
| 55 | 4009.27 | 2720 | | |
| 54 | 4023.99 ⎫ | 3300 | | |
| 18 | 4026.36 ⎭ | | | |
| 16 | 4120.99 | 910 | | |
| 53 | 4143.50 ⎫ | 3150 | | |
| | 4143.76 ⎭ | | | |
| 52 | 4168.97 | 514 | | |
| | 4383.30 ⎫ | 3100 | | |
| | 4387.60 ⎪ | | | |
| 51 | 4387.93 ⎭ | | | |
| 50 | 4437.55 | 542 | | |
| 15 | 4469.92 ⎫ | 4880 | | |
| 14 | 4471.48 ⎪ | | | |
| 14 | 4471.68 ⎭ | | | |
| 12 | 4713.14 ⎫ | 875 | | |
| | 4713.37 ⎭ | | | |
| | 4910.70 ⎫ | 2998 | | |
| 49 | 4920.35 ⎪ | | | |
| 45 | 4921.93 ⎭ | | | |
| C II | | | Yan et al.1987 | |
| 4 | 3918.98 | 35 | -0.551 | 4.6 |
| 4 | 3920.68 | 26 | -0.244 | 5.05 |
| 6 | 4267.02 ⎫ | 76 | 0.558 ⎫ | 4.75 |
| 6 | 4267.27 ⎭ | | 0.734 ⎭ | |
| 39 | 4411.20 | 11 | 0.517 | 4.58 |
| N II | | | Becker & Butler 1989 | |
| 12 | 3995.0 | 30 | 0.225 | 5.23 |
| 48 | 4236.86 ⎫ | 13 | 0.396 ⎫ | 5.03 |
| 48 | 4236.98 ⎭ | | 0.567 ⎭ | |
| 15 | 4447.03 | 9 | 0.238 | 5.32 |
| 5 | 4601.48 | 16 | -0.385 | 4.88 |
| 5 | 4613.8 | 10 | -0.607 | 4.88 |
| 5 | 4630.5 | 26 | 0.093 | 5.13 |

**Table 1.** (continued)

| Ion Mult. | $\lambda$/ Å | $W_\lambda$ / mÅ | Reference $\log gf$ | $-\log n$ |
|---|---|---|---|---|
| O II | | | Becker & Butler 1988 | |
| 6 | 3973.0 | 8 | 0.041 | 5.12 |
| 10 | 4069.62 ⎫ | 24 | 0.149 ⎫ | 4.6 |
| 10 | 4069.89 ⎭ | | -0.245 ⎭ | |
| 10 | 4072.16 | 19 | 0.539 | 4.66 |
| 10 | 4075.86 | 24 | 0.702 | 4.67 |
| 10 | 4078.84 | 10 | -0.249 | 4.22 |
| 19 | 4153.3 | 15 | 0.064 | 4.25 |
| 2 | 4317.14 | 10 | -0.373 | 4.22 |
| 2 | 4319.63 | 8 | -0.367 | 4.76 |
| 2 | 4349.43 | 11 | 0.057 | 4.99 |
| 2 | 4366.86 | 13 | -0.780 | 4.61 |
| 5 | 4414.90 | 27 | 0.241 | 4.58 |
| 5 | 4452.37 | 15 | -0.801 | 4.47 |
| 15 | 4596.17 | 19 | 0.199 | 4.22 |
| 1 | 4649.14 | 24 | 0.340 | 4.82 |
| 1 | 4661.64 | 19 | -0.259 | 4.36 |
| 24 | 4705.36 | 18 | 0.581 | 4.41 |
| Mg II | | | Wiese et al.1969 | |
| 4 | 4481.129 | 58 | 0.732 | 5.48 |
| Al III | | | Kodaira & Scholz 1970 | |
| 3 | 4512.54 | 9 | 0.412 | 6.72 |
| 3 | 4529.18 | 18 | 0.670 | 6.7 |
| Si II | | | Becker & Butler 1990 | |
| 1 | 3856.02 | 14 | -0.418 | 5.49 |
| 1 | 3862.59 | 10 | -0.682 | 5.38 |
| 3 | 4128.05 | 19 | 0.369 | 5.36 |
| 3 | 4130.88 | 18 | 0.545 | 5.56 |
| Si III | | | Becker & Butler 1990 | |
| 2 | 4552.65 | 55 | 0.283 | 5.84 |
| 2 | 4567.87 | 51 | 0.061 | 5.67 |
| 2 | 4574.78 | 19 | -0.416 | 5.76 |
| 9 | 4828.92 | 11 | 0.924 | 5.63 |
| Si IV | | | Becker & Butler 1990 | |
| 1 | 4088.86 | 13 | 0.199 | 5.27 |
| Fe III | | | Kurucz & Pet. 1975 | |
| | 4164.8 | 21 | 0.935 | 5.16 |

## 4. Discussion

*Surface abundances.* Compared with the Sun HD144941 has surface abundances (by number) hydrogen-deficient by 1.7 dex and metal-deficient by 1.6 dex, corresponding to a mass mixture of X=0.014, Y=0.986, Z=0.0003. The determination of the abundances addresses the question of HD144941's fundamental nature and whether it should be classified as an extreme helium star, a helium-rich subdwarf or an intermediate helium star.

Low surface metallicity is unusual amongst EHes, but not amongst the subluminous B stars (sdBs), where it is caused by gravitational settling (Lamontagne et al. 1985). However, settling would also reduce the helium abundance, so unless the star was already extremely H-deficient, the observed high helium abundance argues against the low metallicity being a purely surface phenomenon. Also settling is selectively disrupted by radiative forces, leaving some species (e.g. N) undepleted. The argument against settling is strengthened by the fact that the surface gravity is $> 1$ dex lower than found in sdB stars, thus the low metallicity is probably primordial.

Similarly, the H abundance is much lower than found in any intermediate helium star (Hunger 1975). The latter are consid-

**Table 2.** Photospheric parameters and abundances derived from fine analysis with values for a number of comparison stars - HD144941 (Harrison & Jeffery this paper), the Sun (Anders & Grevesse 1989), the extreme helium stars V652 Her (Lynas-Gray et al. 1984, Jeffery et al. 1986) and LSS3184 (Drilling et al. 1996) and the helium rich sub-dwarf B star PG1544+487 (Heber et al. 1988)

| | HD144941 | | | Sun | PG1544 +487 | LSS3184 | V652 Her |
|---|---|---|---|---|---|---|---|
| $T_{\rm eff}$ / kK | $23.2 \pm 0.5$ | | | 5.78 | 31.0 | 23.2 | 23.5 |
| $\log(g\,/\,cm\,s^{-2})$ | $3.9 \pm 0.2$ | | | 4.44 | 5.1 | 3.4 | 3.7 |
| Abundance | % (by number) | log n | [X] | log n (normalised to $\log \sum n\mu = 12.15$) | | | |
| H | *5.21* | $10.28 \pm 0.20$ | -1.7 | 12.0 | 9.0 | 8.14 | 9.5 |
| He | *94.78* | 11.54 | +0.6 | 10.99 | 11.54 | 11.54 | 11.54 |
| C | *0.00172* | $6.80 \pm 0.19$ | -1.8 | 8.56 | 9.5 | 9.02 | 7.03 |
| N | *0.000788* | $6.46 \pm 0.17$ | -1.6 | 8.05 | | 8.39 | 8.93 |
| O | *0.00244* | $6.95 \pm 0.25$ | -2.0 | 8.93 | | 8.02 | 7.91 |
| Mg | *0.000314* | $6.06 \pm 0.20$ | -1.5 | 7.58 | | 7.17 | 8.13 |
| Al | *0.0000185* | $4.83 \pm 0.20$ | -1.6 | 6.47 | | 6.04 | 6.70 |
| Si | *0.000267* | $5.99 \pm 0.18$ | -1.6 | 7.55 | | 6.84 | 7.71 |
| Fe | *0.000656* | $6.38 \pm 0.25$ | -1.1 | 7.48 | | | |

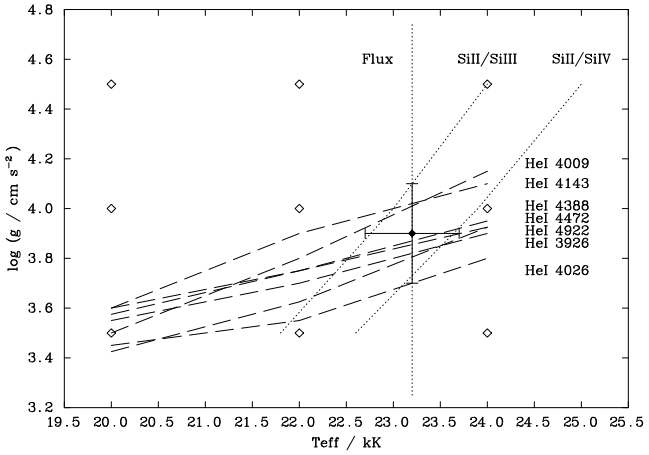


**Fig. 4.** The loci of HeI line profile fits, ionisation equilibria and Flux distribution analysis in $T_{\rm eff}$–$\log g$ space. Unfilled diamonds indicate the grid of model atmospheres used. The solid diamond represents the set of parameters selected for the final model

ered to be population I main-sequence B stars in which strong magnetic fields have disturbed the surface composition. With Z=0.0003 and $\log g$ = 3.9, HD144941 is too old and too luminous to be a near main-sequence B star. Whilst above average for an EHe star, the H abundance is less than that found in the EHe star DY Cen (Jeffery & Heber 1993).

Whilst these arguments point towards HD144941 being an EHe with a very low initial metallicity, the metal abundances present a further difficulty in not showing the products of any nuclear reactions other than hydrogen burning. Typically C and N are enhanced in most other EHes. Once again, there are exceptions, with V652 Her (Jeffery et al. 1986) and MV Sgr (Jeffery et al. 1988) not showing significant C enrichment. If anything, there is weak evidence for C and O depletion in HD144941, but it is an open question whether this is evidence for CNO cycled material.

*Pulsation.* Sufficiently luminous He stars are known to pulsate across a wide range of $T_{\rm eff}$. Additionally the low luminosity stars LSS3184 and V652 Her have been found to pulsate. Calculation of new opacities taking better account of heavy elements has led Saio (1996) to predict that instability against radial pulsation can exist in low luminosity early B stars within a small $T_{\rm eff}$ range. The pulsations are driven by high opacity in metal ionizing layers ($T \sim$ 20kK), so the stability against pulsation decreases with increasing metallicity (Fig. 5).

The values of $T_{\rm eff}$ and $\log g$ derived for HD144941 place it above the boundary and within the instability 'finger' for $Z$ = 0.01 but below the boundary for $Z$ = 0.004. The measured metallicity of $Z$ = 0.0003 is sufficiently low that radial pulsations are not expected to be excited in HD144941. The observational verification of this result (Jeffery & Hill 1996) is a vindication of the pulsation models and opacities.

*Evolution.* The most likely scenarios for the origins of EHes are the last thermal pulse in a post-AGB star (LTP: Iben et al. 1983) and the merger of a CO and He binary white dwarf (MBWD: Webbink 1984). A crucial test of these scenarios will be a comparison of the surface abundances that are observed and those that are predicted by detailed calculations. Evidently these calculations must allow considerable latitude in the range of final abundances for several species. Both scenarios may face difficulties in accounting for HD144941, with its helium enriched and otherwise unprocessed metal-poor atmosphere.

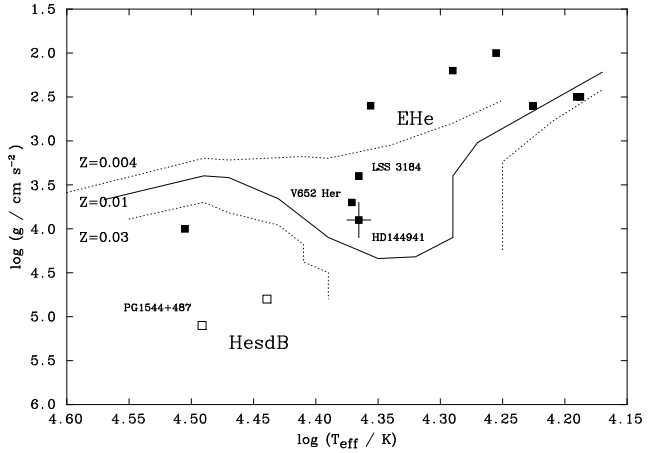


**Fig. 5.** The log $g$-$T_{\rm eff}$ diagram for known EHe and HesdB stars showing the position of HD144941. Instability boundaries (Saio 1996) are shown for $M = 0.7\,{\rm M}_{\odot}$ and varying metallicity, Z. A star is predicted to be unstable if it lies above the line for its relative metallicity

## 5. Conclusion

An analysis of the absorption lines in the optical spectrum of HD144941 has been carried out using LTE atmospheric models. The derived values of $T_{\rm eff}$ = 23.2kK and $\log g$ = 3.9 place HD144941 at the high $T_{\rm eff}$ , high $\log g$ end of the EHe group close to the HesdB stars (Fig. 5).

Surface abundances have been calculated from available species' equivalent widths giving a mass mixture of X=0.014, Y=0.986, Z=0.0003. HD144941 is unusual both for its extremely low metallicity and its high H abundance (compared to a typical EHe). The intermediate surface gravity is too low for gravitational settling to play a significant rôle in HD144941. The low metal abundance (Z=0.0003) is therefore probably of primordial origin. The hydrogen abundance ( $n_{\rm H}/\,n_{\rm He}$ = 0.055) is lower than that of an intermediate helium star. Also, HD144941 is too old and too luminous to be a population I B star like an intermediate helium star. It is most likely that HD144941 is an EHe in which He, but no other species, has been brought to the surface.

The new values of $T_{\rm eff}$ and $\log g$ make HD144941 an ideal candidate for a radial pulsator. The observed low metallicity explains why it is observed to be non-variable and stable against radial pulsation.

*Acknowledgements.* We would like to thank Dr H Saio for kindly making his pulsational data available to us before its publication. Data reduction was carried out using Starlink software. Model atmospheres and synthetic spectra were calculated using CCP7 software. PMH is funded by PPARC. CSJ is funded by CCP7.

## References

Anders E., Grevesse N., 1989. Geochim. Cosmochim. Acta, 53, 197.
Barnard A.J., Cooper J., Shamey L.J., 1969. A&A 1, 28.
Barnard A.J., Cooper J., Smith E.W., 1974. JQSRT 14, 1025.
Barnard A.J., Cooper J., Smith E.W., 1975. JQSRT 15, 429.
Beauchamp A., Wesemael F., Bergeron P., Liebert J., Saffer R.A., 1996. Hydrogen Deficient Stars, eds. C.S.Jeffery & U.Heber, PASPC 96, 295.
Becker S.R., Butler K., 1988. A&A 201, 232.
Becker S.R., Butler K., 1989. A&A 209, 244.
Becker S.R., Butler K., 1990. A&A 235, 326.
Butler K., 1984. PhD Thesis, University of London.
Drilling J.S., 1986. IAU Coll. 87, Hydrogen Deficient Stars and Related Objects, eds. K.Hunger, D.Schönberner & N.K.Rao, ASSL 128, 9.
Drilling J.S., Jeffery C.S. Heber U., 1996. Hydrogen Deficient Stars, eds. C.S.Jeffery & U.Heber, PASPC 96, 172.
Harrison P.M., Jeffery C.S., 1996. Hydrogen Deficient Stars, eds. C.S.Jeffery & U.Heber, PASPC 96, 173.
Heber U., Dreizler S., de Boer K.S., Moehler S. and Richtler T., 1988. Astron. Ges. Abs. Ser. 1, 16.
Hunger K., 1975. Problems in Stellar Atmospheres and Envelopes, eds. B.Baschek, W.H.Kegel & G.Traving, Springer, 57.
Hunger K., Kaufmann J.P., 1973. A&A 25, 261.
Iben I., Jr., Kaler J.B., Truran J.W., Rednzini A., 1983. ApJ 264, 605.
Jeffery C.S., Heber U., 1992. A&A 260, 133.
Jeffery C.S., Heber U., 1993. A&A 270, 167.
Jeffery C.S., Hill P.W., 1996. The Observatory 116, 156.
Jeffery C.S., Heber U., Hamann W.R., 1987. New Insights in Astrophysics, ESA SP-263, 369.
Jeffery C.S., Heber U., Hill P.W., 1986. IAU Coll. 87, Hydrogen Deficient Stars and Related Objects, eds. K.Hunger, D.Schönberner & N.K.Rao, ASSL 128, 101.
Kodaira K., Scholz M., 1970. A&A 6, 93.
Kurucz R.L., 1970. ATLAS: A Computer Program for calculating Model Stellar Atmospheres, SAO Special Report No. 309, Cambridge, Massachussets 02138.
Kurucz R.L., Petryemann, E., 1975. A Table of Semiempirical gf values, SAO Special Report No. 362, Cambridge, Massachussets 02138.
Lamontagne R., Wesemael F., FontaineG., Sion E.M., 1985. ApJ 299, 496.
Lynas-Gray A.E., Schönberner D., Hill P.W., Heber U., 1984. MNRAS 209, 387.
MacConnell D.J., Frye R.L., Bidelman W.P., 1970. PASP 82, 730.
Mengel J.G., Sweigart A.V., Demarque P., Gross P.G., 1979. ApJS 40, 733.
Michaud G., 1987. IAU Coll. 95, Second Conference on Faint Blue Stars, eds. A.G.Philip, D.S.Hayes & J.W.Liebert, L.Davis Press Inc., 249.
Moehler S., Richtler T., de Boer K.S., Dettmar R.J., Heber U., 1990. A&AS 86, 53.
Möller R.U., 1990. Diplom. Thesis, Universität Kiel.
Osmer P.S., Peterson D.M., 1974. ApJ 187, 117.
Peach G., 1970. Mem. R. Astr. Soc. 73, 1.
Saio H., 1996. Hydrogen Deficient Stars, eds. C.S.Jeffery & U.Heber, PASPC 96, 361.
Seaton M.J., 1979. MNRAS 187, 73.
Underhill A.B., 1982. ApJ 263, 741.
Webbink R.F., 1984. ApJ 277, 355.
Wiese W.L., Smith M.W., Miles B.M., 1969. Atomic Transition Probabilities, National Bureau of Standards, Washington.
Yan Y., Taylor K.T., Seaton M.J., 1987. J.Phys.B 20, 6399.

This article was processed by the author using Springer-Verlag LaTeX A&A style file *L-AA* version 3.